Unequivocal signatures of the crossover to Anderson localization in realistic models of disordered quasi-one-dimensional materials

Alejandro Lopez-Bezanilla, Luis S. Froufe-Pérez, Stephan Roche, and Juan José Sáenz

Phys. Rev. B **98**, 235423 — Published 20 December 2018

DOI: 10.1103/PhysRevB.98.235423

Unambiguous Signatures of the Crossover to Anderson Localization in Realistic Models of Disordered Quasi-1D Materials

Alejandro Lopez-Bezanilla,[1] Luis S. Froufe-Pérez,[2] Stephan Roche,[3,4] and Juan José Sáenz[5,6]

[1] *Theoretical Division, Los Alamos National Laboratory, Los Alamos, New Mexico 87545, USA**
[2] *Department of Physics, University of Fribourg, CH-1700 Fribourg, Switzerland*
[3] *Catalan Institute of Nanoscience and Nanotechnology (ICN2), CSIC and The Barcelona Institute of Science and Technology, Campus UAB, Bellaterra, 08193 Barcelona, Spain*
[4] *Institució Catalana de Recerca i Estudis Avançats (ICREA), 08070 Barcelona, Spain*
[5] *Donostia International Physics Center (DIPC), Paseo Manuel Lardizabal 4, 20018 Donostia-San Sebastian, Spain 4*
[6] *IKERBASQUE, Basque Foundation for Science, 48013 Bilbao, Spain*

The only unambiguous known criterion for single-parameter scaling Anderson localization relies on the knowledge of the full conductance statistics. To date, theoretical studies have been restricted to model systems with symmetric scatterers, hence lacking universality. We present an in-depth statistical study of conductance distributions P(g), in disordered 'micrometer-long' carbon nanotubes using first principles simulations. In perfect agreement with the Dorokov-Mello-Pereyra-Kumar scaling equation, the computed P(g) exhibits a non-trivial, non-Gaussian, crossover to Anderson localization which could be directly compared with experiments.

Keywords: Anderson localization, Conductance distribution, Random matrix theory, Scaling theory

I. INTRODUCTION

Anderson localization (AL) is a fundamental mechanism that drives a physical system to an insulating regime due to disorder-induced wave interferences[1]. However, despite five decades of theoretical studies of AL in electronic, photonics and phononic systems[1–6], compelling evidences of AL transition criterion in realistic materials remains challenging[2].

Our current understanding of wave transport through disordered media is mainly founded on the hypothesis of single-parameter scaling (SPS)[8]. According to the SPS hypothesis and in absence of inelastic scattering, the statistical properties of transport are governed by the averaged conductance, $\langle G\rangle = G_0\langle g\rangle$, as a *single scaling parameter* ($G_0 = 2e^2/h$ is the quantum of conductance). Beyond the localization threshold, $\langle g\rangle \lesssim 1$, the Ohmic regime breaks down and $\langle g\rangle$ decreases exponentially with the system size. As opposed to three-dimensional conductors where SPS predicts a disorder-induced metal-insulator transition, in two-dimensional systems and quasi-one-dimensional (Q1D) wires there is a crossover region between the metallic and insulating regimes with a smooth behavior of the conductance mean, $\langle g\rangle$, and variance ($\mathrm{var}\{g\} = \langle g^2\rangle - \langle g\rangle^2$)[9], which makes difficult to identify the onset of the localization regime. In contrast, statistical conductance distributions, $P(g)$, were predicted to exhibit a non-trivial crossover between the diffusive and localized regimes[10–12] with a peculiar shape at the onset of the localized regime. This corresponds to a conductance average $\langle g\rangle \sim 1/2$ with a marked discontinuity in the first derivative of the distribution and a sharp cutoff beyond $g = 1$[13]. These predictions have been corroborated with numerical results on different model systems in both Q1D[10,14] and two-dimensional disordered systems[15,16]. Strong deviations from both Gaussian and log-normal distributions had also been observed in the metal-insulator transition in three dimensions[6,17].

However, there is still neither direct experimental evidence of this crossover nor comparison with numerical simulations based on quantum wires with realistic disorder, such as that introduced by foreign species and structural modifications. Although approaches combining the accuracy of first-principles methods with the scaling analysis of charge transport properties at the mesoscale are allowing for improved predictions of complex system's behavior[7], theoretical understanding of the observed quantum interference phenomena is still far from being complete.

Previous simulations on realistic models of B- and P-doped silicon nanowires using first-principles simulations[18] showed a transition from ballistic to diffusive regime where both sample-averaged conductance, $\langle g\rangle$, and sample-to-sample fluctuations[19], were in good agreement with the predictions of SPS: the statistical averages where shown to only depend on the ratio $s \equiv L/\ell$ between the nanowire's length, L, and the mean free path, ℓ, (which depends on the scattering properties of a single dopant). Based on an exponential decrease of the averaged conductance with the wire's length, Anderson localization was reported in irradiated nanotubes at room temperature[20] in agreement with first principles calculations of carbon nanotubes with vacancies[21]. However, the identification of regions where conductance decreases exponentially neither reveals the actual physical mechanism behind this rapid drop, nor necessarily implies Anderson localized states. *Tunneling* of electrons through *localized* defect-induced states[22–24] (or absorption channels in the case of light transport[25]) can also lead to an

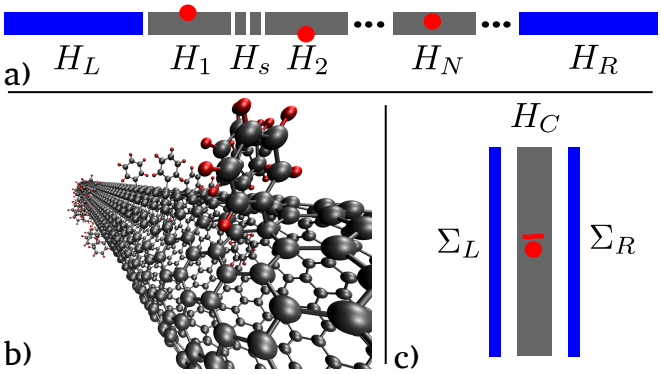

FIG. 1. a) Schematic representation of a disordered channel attached to two semi-infinite electrodes. Defected tube sections (represented by H_N Hamiltonian matrices) are assembled in a random arrangement with clean spacer sections (H_s). The two probe device is completed with the channel attached to left (H_L) and right (H_R) electrodes. b) Ball-stick representation of a nanotube with phenyl rings attached to the sidewall. c) Effective model of the device where the self-energies of the left (Σ_L) and right (Σ_R) electrodes are in contact with a renormalized channel H_C.

exponential drop but with statistical signatures very different from the SPS predictions based on the interference between *propagating* scattered waves.

In this Letter, the predicted non-trivial crossover from diffusion to Anderson localization is demonstrated with a realistic defective quantum waveguide, such as chemically modified carbon nanotubes (CNTs), which are exactly reproduced by the Dorokov-Mello-Pereyra-Kumar (DMPK) equation[26,27]. A computational study of charge transport in metallic single-walled CNTs with random distribution of paired phenyl groups bonded to the tube sidewalls using the Landauer-Büttiker (LB) formalism is first presented. Specifically we consider modified metallic armchair CNT(6,6) and CNT(10,10) tubes of varying defect density. A crossover from quasi-ballistic to diffusive and Anderson localized transport is analyzed using statistical conductance distributions. The results are exactly reproduced with highly non-trivial non-Gaussian functions which unambiguously identify the precise dominating transport length scale that dictates the downscaling behavior of the conductance.

II. RESULTS AND DISCUSSION

A. First-principles scheme

The nanowire is divided in a scattering region (defective CNT), where charge carriers are backscattered during their propagation, coupled to two semi-infinite electrodes (pristine CNTs) with reflectionless contacts as sketched in Fig. 1. The geometry optimizations and electronic structure calculations were performed with the density functional theory (DFT) based SIESTA code[28,29]. A double-ζ polarized basis set within the local density approximation approach for the exchange-correlation functional was used. CNTs were modeled within a supercell large enough to allow the nanotube extremes to converge to the unperturbed system, avoiding interactions between neighboring cells. Thus, functionalized and clean sections of CNTs can match and long systems with perfect contact areas between the building blocks can be built up (Fig.1a-b). Random arrangements of modified and pristine sections mimic rotational and translational disorder. A real-space renormalization procedure allows for finding an effective Hamiltonian representation of the channel within the accuracy of the first-principles calculations[7,30] A set of first-principles calculations were first performed to obtain the Hamiltonians (H) and overlap (S) matrices of CNT segments whose wall was modified by external groups. The integration over the Brillouin zone was performed using a Monkhorst sampling of 1×1×4 k-points for chemically modified 14-primitive armchair unit cell long tubes. The radial extension of the orbitals had a finite range with a kinetic energy cutoff of 50 meV. The numerical integrals were computed on a real-space grid with an equivalent cutoff of 300 Ry. Atomic positions were relaxed with a force tolerance of 0.02 eV/Å.

B. Conductance calculations

Charge transport properties of modified CNTs are analyzed within the LB formulation of the conductance[30–34], which is particularly appropriate to study charge motion along a Q1D device channels. At quasi-equilibrium conditions, i.e. small bias voltages, the LB conductance is given by $g(E_F) = \sum_n T_n(E_F)$, where the sum runs over all the propagating charge carrier channels. The transmission coefficients $T_n(E_F)$ give the probability of a charge carrier at the Fermi level, E_F, to be transmitted from channel n of one electrode to the opposite electrode. The conductance can also be written in terms of the retarded (advanced) Green function $\mathcal{G}^+(E)$ ($\mathcal{G}^-(E)$),

$$\mathcal{G}^{\pm}(E) = \{E\ \mathrm{S} - \mathrm{H} - \Sigma_L^{\pm}(E) - \Sigma_R^{\pm}(E)\}^{-1} \qquad (1)$$

where $\Sigma^{\pm}_{L(R)}(E)$ is the self-energy describing the coupling of the channel to the left (right) electrode (Fig.1c). The dimensionless conductance g of the system in the standard Green function formalism[35] is then given by

$$g = \sum_{n=1}^{N} T_n(E_F) = \mathrm{trace}\Big\{\Gamma_L \mathcal{G}^+ \Gamma_R \mathcal{G}^-\Big\}_{E=E_F}. \qquad (2)$$

Green functions associated with the H and S matrices are used in a real-space normalization procedure to include recursively the contribution of the sections within an O(N) scheme with respect to the tube length, and with no loss of the first-principles accuracy.

In the absence of impurities, $T_n(E) = 1$, and g is quantized and equal to the total *integer* number, N, of open

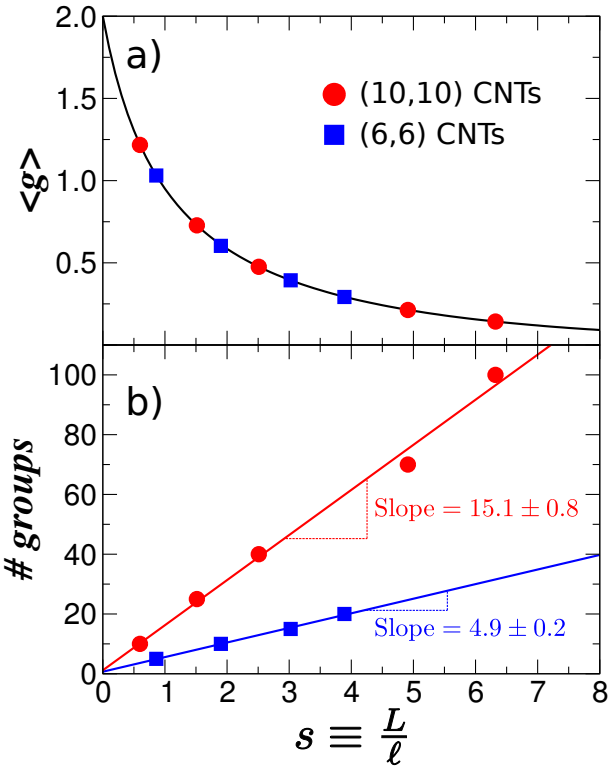

FIG. 2. a DMPK averaged conductance $\langle g\rangle$ versus the normalized CNT length s (full line) together with the DFT averages for CNTs (10,10) (circles) and (6,6) (squares) with different number of attached groups. Each symbol is shifted to a value of $s = L/\ell$ such that it lies on the DMPK curve. b number of groups as a funciton of the normalized length s for (10,10) and (6,6) CNTs (same symbols as in a). Lines are the corresponding linear regressions for each data set

propagating modes at the energy E_F. The orbitals rearrangement due to the covalent attachment of phenyl groups can lead to a significant reduction of the transmission coefficients. The transmission spectrum for a broad range of energies of CNTs with phenyl groups attached to the sidewall has been discussed in detail[7]. We shall focus on the statistical properties of the conductance as a function of the linear density of scatterers, $\rho = N_g/L$ (N_g is the number of attached groups). For each scatterer density, ρ, transport calculations based on the first-principles derived model were performed over 2000 different random distributions of groups on $L = 1\mu m$ length CNTs.

C. DMPK equation and scaling theory

The expected results from SPS theory are here briefly summarized. A quantitative description for transport fluctuations in Q1D systems is given by the DMPK equation[26,27] and by the field-theoretic approach due to Efetov and Larkin[36] (shown to be equivalent to DMPK[37]). For a general discussion about the DMPK

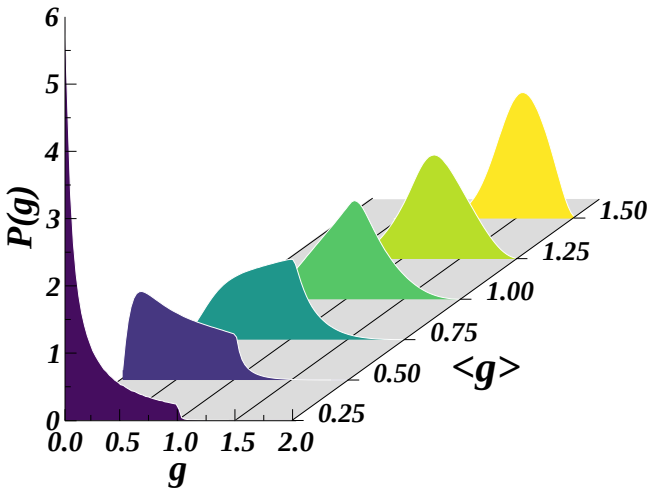

FIG. 3. Conductance distributions in the DMPK model for different values of the averaged conductance in a two propagating channels disordered system.

equation the reader is referred to refs.[3,5]. In Figure 2(a), $\langle g\rangle$ versus $s = L/\ell$ obtained from the numerical solution of the DMPK equation for $N = 2$ channels[12,14] is plotted. For wire's lengths shorter than the localization length, $\xi \sim (N+1)\ell = 3\ell$ (i.e. $s \lesssim 3$), the conductance drops as

$$\langle g\rangle \sim \frac{N}{1+s}. \tag{3}$$

At fixed $L = 1\ \mu m$ and within the LB scheme, averaged conductances for a number of defects from $N_g = 5$ up to 100 were computed. According to standard transport theory, in absence of spatial correlations, $\ell^{-1} = \rho\langle\sigma\rangle = (N_g/L)\langle\sigma\rangle$, where $\langle\sigma\rangle$ is the averaged scattering cross section of a single scatterer which is a dimensionless quantity in Q1D systems. This gives

$$s = \frac{L}{\ell} = \langle\sigma\rangle N_g. \tag{4}$$

Assuming that $\langle g\rangle$ is the scaling parameter, the DMPK results can be used to obtain $\langle\sigma\rangle$ from the LB formalism results for $\langle g\rangle$. The expected linear behavior based on equation (4) is demonstrated in Fig. 2(b). Our results demonstrate that the scattering cross section of a single scatterer in a CNT(6,6) ($\langle\sigma\rangle \sim 1/5$) is 3 times stronger than in a CNT(10,10) ($\langle\sigma\rangle \sim 1/15$).

D. Conductance distributions

While the statistical averages show no trace of the crossover region from diffusion to localization, the nontrivial crossover can be clearly seen in the DMPK conductance distributions as illustrated in Fig 3. $P(g)$ were calculated from a Monte Carlo sampling of the joint probability distribution of two transport eigenchannels given

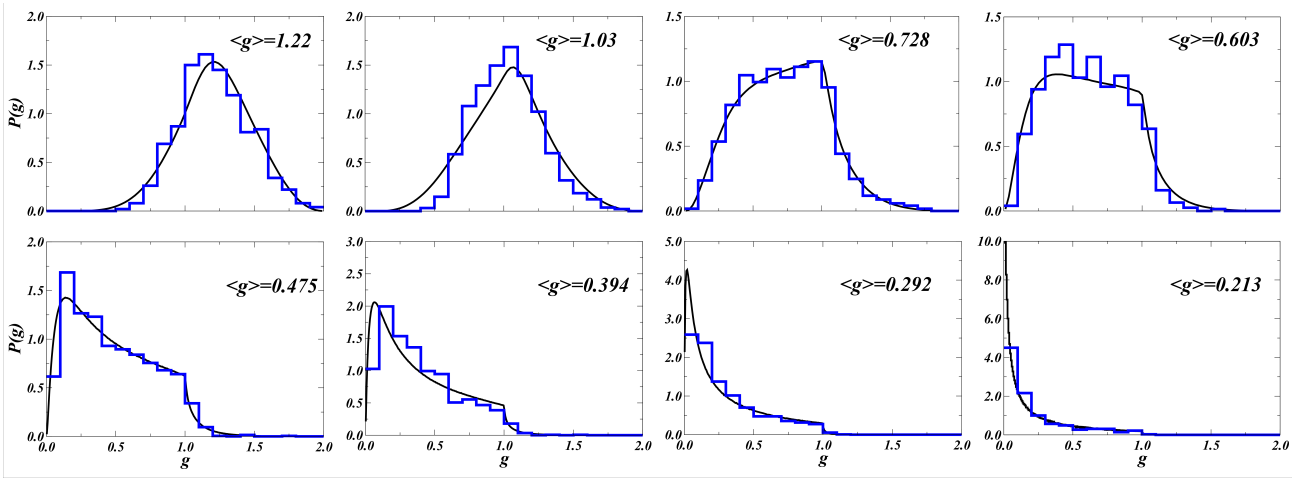

FIG. 4. Conductance distribution plots for CNTs with an increasing number (from 5 up to 100) of functional groups. Statistical distributions were performed over 2000 random configurations. Lines correspond to the DMPK distributions.

by the DMPK model[14]. The conductance distributions computed from first-principles derived model are plotted in Fig. 4 together with the DMPK results obtained for the same $\langle g \rangle$ values. There is a clear one-to-one correspondence between the former calculations and the DMPK predictions.

This demonstrate that transport in a quantum waveguide with realistic disorder is controlled by a single scaling parameter, i.e. the averaged conductance, and that macroscopic transport properties can be obtained through the scattering properties of a single defect. CNTs with only two conducting channels were shown to exhibit an unambiguous signature of the non-trivial crossover from diffusion to Anderson localization regimes as predicted from the DMPK scaling approach. Interestingly, this signature differs from the one observed on model-system wires with surface defects[10].

III. CONCLUSIONS

Our results show that, in a more general case of disorder features, a rigorous evaluation of fundamental transport length scales (mean free path and localization lengths) can be unequivocally determined, thus enabling to determine the dominating transport regime for a given material characteristics (defect density, material geometry,...). This should stimulate further experimental exploration of conductance statistics to access the actual transport length scales through the Anderson localization transition analysis.

IV. ACKNOWLEDGMENTS

This work was supported by the U.S. Department of Energy, and by the Spanish Ministerio de Economía y Competitividad and European Regional Development Fund (Grant No. FIS2015-69295-C3-3-P).

* alejandrolb@gmail.com

[1] P. W. Anderson, Phys. Rev. **109**, 1492 (1958).
[2] E. Abrahams, *50 years of Anderson Localization*, Vol. 24 (World Scientific, 2010).
[3] P. A. Mello and N. Kumar, *Quantum transport in mesoscopic systems: complexity and statistical fluctuations, a maximum-entropy viewpoint*, 4 (Oxford University Press on Demand, 2004).
[4] E. Akkermans and G. Montambaux, *Mesoscopic physics of electrons and photons* (Cambridge University Press, 2007).
[5] C. W. J. Beenakker, Rev. Mod. Phys. **69**, 731 (1997).
[6] P. Markoš, Acta Physica Slovaca **56**, 561 (2006).
[7] A. Lopez-Bezanilla, F. Triozon, S. Latil, X. Blase, and S. Roche, Nano Lett. **9**, 940 (2009).
[8] E. Abrahams, P.W. Anderson, D.C. Licciardello, and T.V. Ramakrishnan, Phys. Rev. Lett. **42**, 673 (1979).
[9] A. D. Mirlin, A. Müller-Groeling, and M. R. Zirnbauer, Ann. Phys. **236**, 325 (1994).
[10] A. García-Martín and J. J. Sáenz, Phys. Rev. Lett. **87**, 116603 (2001).
[11] K. Muttalib, P. Wölfle, A. Garcia-Martin, and V. Gopar, EPL (Europhysics Letters) **61**, 95 (2003).
[12] L. S. Froufe-Pérez, P. García-Mochales, P. A. Serena, P. A. Mello, and J. J. Sáenz, Phys. Rev. Lett. **89**, 246403 (2002).
[13] K.A. Muttalib and P. Wölfle, Phys. Rev. Lett. **83**, 3013 (1999).
[14] L.S. Froufe-Pérez, M. Yépez, P.A. Mello, and J.J. Sáenz, Phys. Rev. E **75**, 031113 (2007).

[15] A.M. Somoza, J. Prior, M. Ortuno, and I.V. Lerner, Phys. Rev. B **80**, 212201 (2009).

[16] L. S. Froufe-Pérez, M. Engel, J. J. Sáenz, and F. Scheffold, Proceedings of the National Academy of Sciences , 201705130 (2017).

[17] K. Slevin and T. Ohtsuki, Phys. Rev. Lett. **78**, 4083 (1997); C. M. Soukoulis, X. Wang, Q. Li, and M. M. Sigalas, *ibid.* **82**, 668 (1999).

[18] T. Markussen, R. Rurali, A.-P. Jauho, and M. Brandbyge, Phys. Rev. Lett. **99**, 076803 (2007).

[19] P. A. Lee and A. D. Stone, Phys. Rev. Lett. **55**, 1622 (1985).

[20] C. Gómez-Navarro, P. De Pablo, J. Gómez-Herrero, B. Biel, F. Garcia-Vidal, A. Rubio, and F. Flores, Nat. Mater. **4**, 534 (2005).

[21] B. Biel, F. J. García-Vidal, A. Rubio, and F. Flores, Phys. Rev. Lett. **95**, 266801 (2005).

[22] E. Medina and M. Kardar, Phys. Rev. B **46**, 9984 (1992).

[23] L. I. Deych, A.A. Lisyansky, and B.L. Altshuler, Phys. Rev. B **64**, 224202 (2001).

[24] J. Prior, A.M. Somoza, and M. Ortuno, Phys. Rev. B **72**, 024206 (2005).

[25] S. Skipetrov and J. H. Page, New J. Phys. **18**, 021001 (2016).

[26] O. Dorokhov, JETP Lett **36**, 318 (1982).

[27] P. Mello, P. Pereyra, and N. Kumar, Ann. Phys. **181**, 290 (1988).

[28] P. Ordejón, E. Artacho, and J. M. Soler, Phys. Rev. B **53**, R10441 (1996).

[29] J. M. Soler, E. Artacho, J. D. Gale, A. García, J. Junquera, P. Ordejón, and D. Sánchez-Portal, J. Phys.: Condens. Matter **14**, 2745 (2002).

[30] B. Biel, F. J. Garcia-Vidal, A. Rubio, and F. Flores, J. Phys.: Condens. Matter **20** (2008).

[31] A. López-Bezanilla, F. Triozon, S. Latil, X. Blase, and S. Roche, Nano Lett. **9**, 940 (2009).

[32] F. Teichert, A. Zienert, J. Schuster, and M. Schreiber, J. Comput. Phys. **334**, 607 (2017).

[33] F. Teichert, A. Zienert, J. Schuster, and M. Schreiber, Computational Materials Science **138**, 49 (2017).

[34] D. Teich, M. Claus, and G. Seifert, J. Comput. Electron. (2018).

[35] D. S. Fisher and P. A. Lee, Phys. Rev. B **23**, 6851 (1981).

[36] K. Efetov and A. Larkin, Sov. Phys. JETP **58**, 444 (1983).

[37] P.W. Brouwer and K. Frahm, Phys. Rev. B **53**, 1490 (1996).